IEEE Access
Multidisciplinary | Rapid Review | Open Access Journal

Received September 13, 2018, accepted October 1, 2018, date of publication October 8, 2018, date of current version October 31, 2018.

Digital Object Identifier 10.1109/ACCESS.2018.2874625

Anticipation in the Polarization Chaos Synchronization of Uni-Directionally Coupled Vertical-Cavity Surface-Emitting Lasers With Polarization-Preserved Optical Injection

ELUMALAI JAYAPRASATH[1], YU-SHUANG HOU[1,2], ZHENG-MAO WU[1], AND GUANG-QIONG XIA[1]

[1]School of Physics, Southwest University, Chongqing 400715, China
[2]School of Science, Inner Mongolia University of Science and Technology, Baotou 014010, China

Corresponding authors: Zheng-Mao Wu (zmwu@swu.edu.cn) and Guang-Qiong Xia (gqxia@swu.edu.cn)

This work was supported by the National Natural Science Foundation of China under Grant 61475127, Grant 61575163, Grant 61775184, and Grant 61875167.

ABSTRACT We investigate numerically the anticipated synchronization in the two uni-directionally coupled vertical-cavity surface-emitting lasers (VCSELs) as master and slave configuration. The master VCSEL is rendered chaotic state by an isotropic optical feedback and master's chaotic output uni-directionally injected to a slave VCSEL under polarization-preserved optical injection. The synchronization quality and lag time between lasers are obtained by performing cross-correlation analysis. When the laser's parameters are identical, a regime of anticipatory synchronization is found in both of the linearly polarized mode dynamics of the master and slave lasers, if the feedback delay time is greater than the coupling time. Anticipation is robust to a small variation in injection rate, frequency detuning, and laser's internal parameter mismatches, but the synchronization is not complete. Injection-locking synchronization regime occurs between master and slave lasers for higher injection, positive detuning, and larger mismatch in the internal parameters. We show the mapping of synchronization quality, sustenance of anticipatory synchronization and switching of regimes in the injection rate and parameter mismatch plane. The anticipation maintained even for higher injection rates if mismatch is introduced in certain internal parameters.

INDEX TERMS Anticipation, chaos synchronization, injection-locking, vertical-cavity surface-emitting lasers.

I. INTRODUCTION

In recent times, vertical-cavity surface emitting lasers (VCSELs) are auspicious diode lasers due to their several advantages and desirable characteristics such as low threshold current, circular symmetry output with narrow diverging profile, and easy to photonic integration. These great advantages of VCSELs have made considerable development and used in many applications as compared with the conventional edge-emitting lasers [1]–[5]. Moreover, VCSEL has the tendency to emit linearly polarized (LP) light in one of two orthogonal directions (x-LP and y-LP). The VCSEL light output may easily switch between x-LP and y-LP modes, which is polarization switching (PS), as the laser operating conditions such as temperature or bias current are varied. Two types of PS, type I PS (from y polarization mode with high frequency to x polarization mode with low frequency) and type II PS (from x-LP low frequency to y-LP high frequency), in VCSELs have been discussed. Several theoretical and experimental studies on PS have been carried out for both to understand the physical mechanism and for the development of polarization control techniques and applications [6]–[11]. Besides, complex dynamics arises in VCSEL light output when the laser is subject to optical feedback [12], [13], to injection from another laser [14], [15], or to current modulation [16], [17].

Considerable research has been focused and devoted on VCSELs chaotic light source based secure optical communications [18]–[21]. The fundamental idea of secure optical communications is to use the transmitter's chaotic output to encode a message and transmit to a receiver.

Synchronizing transmitter and receiver is an essential condition so as to decode the message at the receiver [22]–[24]. Chaos synchronization has been demonstrated in nonlinear systems [25] and in several laser systems, including gas (CO_2) [26], Nd:YAG [27], erbium-doped fiber ring lasers [28], NH_3 [29], solid-state [30], edge-emitting diode lasers [31], and VCSELs [32], [33]. In the coupled lasers system consisting of a semiconductor laser (master laser) subject to optical feedback by an external cavity reflector so as to obtain chaotic output, where the external-cavity round-trip time is τ. And the chaotic output is injected into another semiconductor laser (slave laser), the coupling time between master and slave laser is τ_c. Chaos synchronization depends on the lag time arising due to the slave laser dynamics. Essentially this lag time is known as retardation time [34]–[36]. In 2000, Voss analytically found a regime of anticipation synchronization when τ is greater than τ_c, i.e., the slave laser anticipates the chaotic dynamics of master laser by an amount of $\tau - \tau_c$ time [37]. When τ is less than τ_c, retarded synchronization occurs where the slave chaotic dynamics lags with the master laser dynamics by an amount of $\tau_c - \tau$ time. Ahlers *et al.* has reported the retarded chaos synchronization in uni-directionally coupled two external-cavity semiconductor lasers [38]. Masoller has numerically carried out the anticipation synchronization in chaotic semiconductor lasers subject to optical feedback [39]. Experimental demonstration of anticipating synchronization [40] and a detailed characterization of anticipation and retarded synchronization in external cavity semiconductor lasers had been reported [41].

In VCSELs, the first numerical studies of chaos synchronization under master-slave configuration have been reported by Spencer *et al.* [42]. The focus was on the total intensity of the VCSEL and not considered polarization dynamics. Chaos synchronization in uni-directionally and mutually coupled VCSELs have been experimentally demonstrated [32], [33]. The practical application of chaotic VCSELs in secure communication has been demonstrated in 2004 [18]. Many theoretical and experimental studies on chaos synchronization in two coupled VCSELs under uni-directional and mutual coupling configuration have been reported [43]–[49]. Besides, synchronization of vectorial chaos in two coupled VCSELs has also been studied numerically [50]. In uni-directionally coupled multi-transverse mode VCSELs, injection-locking and complete synchronization regimes have been numerically studied in 2004 [43]. When the master and slave lasers are perfectly identical, anticipation with $\tau - \tau_c$ time arises in the complete synchronization regime. And also for higher injection rate, slave dynamics lags master laser dynamics with τ_c time in injection-locking synchronization regime. In 2007, polarization mode competition on chaos synchronization of uni-directionally coupled VCSELs has been numerically reported. Keeping $\tau > \tau_c$ and $\tau_c = 0$, anticipatory synchronization has been studied [44]. Between master and slave, retarded synchronization with $\tau_c - \tau$ time when $\tau < \tau_c$ has been reported in complete synchronization regime of uni-directionally coupled VCSELs [48]. Additionally, anticipating synchronization in mutually coupled VCSELs has been reported numerically and experimentally [51], [52].

In this paper we theoretically analyze the regimes of anticipation and injection-locking synchronization in uni-directionally coupled VCSELs by considering the configurations of a master laser with the isotropic optical feedback from an external cavity reflector and polarization-preserved optical injection to slave laser. The quality of chaos synchronization and lag time are calculated by performing the cross-correlation analysis between the chaotic output of master and slave lasers. The synchronization is characterized by injection rate, frequency detuning, and mismatched parameters of the lasers. We show that, in both linearly polarized modes (x-LP and y-LP) dynamics, the slave laser anticipates master laser by the amount of $\tau - \tau_c$ time, when $\tau > \tau_c$. The anticipated synchronization is robust to a small variation of injection rate, frequency detuning and parameter mismatch, but in this case the synchronization is not complete. We investigate a regime of injection-locking synchronization between master and slave lasers, in which slave lag with τ_c time behind master for higher injection rates, positive detuning, and parameter mismatch. We show that anticipation synchronization is preserved for an adequate injection rate with introducing mismatches in certain internal parameters. These properties of synchronization quality and switching of regimes have been discussed in the plane of injection rate and parameter mismatch.

II. RATE EQUATION MODEL

The laser rate equation model extends the spin flip model for two single-transverse mode VCSELs under uni-directional coupling master-slave configuration [2]. Master laser (ML) is subject to isotropic optical feedback to obtain chaotic output. The ML's chaotic output uni-directionally injected to slave laser (SL) under polarization-preserved optical injection. The rate equations for the master laser

$$\frac{dE_x^m}{dt} = \kappa(1+i\alpha)[(N^m-1)E_{x,}^m + in^m E_y^m] - (\gamma_a + i\gamma_p)E_x^m + fE_x^m(t-\tau)e^{-i\omega_m\tau} + F_x^m \quad (1)$$

$$\frac{dE_y^m}{dt} = \kappa(1+i\alpha)[(N^m-1)E_y^m - in^m E_x^m] + (\gamma_a + i\gamma_p)E_y^m + fE_y^m(t-\tau)e^{-i\omega_m\tau} + F_y^m, \quad (2)$$

$$\frac{dN^m}{dt} = -\gamma[N^m - \mu + N^m(|E_x^m|^2 + |E_y^m|^2)] - i\gamma n^m(E_y^m E_x^{m^*} - E_x^m E_y^{m^*}), \quad (3)$$

$$\frac{dn^m}{dt} = -\gamma_s n^m - \gamma n^m(|E_x^m|^2 + |E_y^m|^2) - i\gamma N^m(E_y^m E_x^{m^*} - E_x^m E_y^{m^*}), \quad (4)$$

and for the slave laser

$$\frac{dE_x^s}{dt} = \kappa(1+i\alpha)[(N^s-1)E_x^s + in^s E_y^s] - (\gamma_a + i\gamma_p)E_x^s + \eta E_x^m(t-\tau_c)e^{-i(\omega_m\tau_c - \Delta\omega t)} + F_x^s, \quad (5)$$

$$\frac{dE_y^s}{dt} = \kappa(1+i\alpha)[(N^s-1)E_y^s - in^s E_x^s] + (\gamma_a + i\gamma_p)E_y^s + \eta E_y^m(t-\tau_c)e^{-i(\omega_m\tau_c - \Delta\omega t)} + F_y^s, \quad (6)$$

$$\frac{dN^s}{dt} = -\gamma[N^s - \mu + N^s(|E_x^s|^2 + |E_y^s|^2)] - i\gamma n^s(E_y^s E_x^{s*} - E_x^s E_y^{s*}), \quad (7)$$

$$\frac{dn^s}{dt} = -\gamma_s n^s - \gamma n^s(|E_x^s|^2 + |E_y^s|^2) - i\gamma N^s(E_y^s E_x^{s*} - E_x^s E_y^{s*}) \quad (8)$$

where the superscripts m and s stand for the ML and SL respectively. $E_{x,y}$ are account for the linearly polarized slowly varying components of the amplitudes, N represents the total carrier inversion between conduction and valence bands, and n is the difference between carrier inversions with opposite spins. κ represents the photon decay rate. γ is the carrier decay rate. γ_s is the spin-flip relaxation rate which accounts for the microscopic processes involved in the homogenization of carrier spin. γ_a and γ_p are the linear anisotropies accounting cavity dichroism and birefringence, respectively. α is the the linewidth enhancement factor. μ corresponds to the normalized injection current (at threshold $\mu = 1$). $\Delta\omega = \omega_m - \omega_s = 2\pi\Delta f$ is the frequency detuning between ML and SL. Here, ω_m (ω_s) is the optical frequency of master (slave) laser at the solitary laser threshold in the absence of linear anisotropies. f is feedback rate, and η is the injection rate. τ is the external-cavity round-trip time. τ_c is the coupling time between master to slave laser. Spontaneous emission noise is modeled by Langevin sources: $F_x^{m,s} = \sqrt{\frac{\beta_{sp}}{2}}(\sqrt{N^{m,s}+n^{m,s}}\xi_1^{m,s} + \sqrt{N^{m,s}-n^{m,s}}\xi_2^{m,s}$ and $F_y^{m,s} = -i\sqrt{\frac{\beta_{sp}}{2}}(\sqrt{N^{m,s}+n^{m,s}}\xi_1^{m,s} - \sqrt{N^{m,s}-n^{m,s}}\xi_2^{m,s})$, with ξ_1 and ξ_2 independent Gaussian white noise with zero mean and unitary variance, and β_{sp} corresponds to the spontaneous emission rate. We use the following parameters fixed for the numerical integration: $\kappa = 300\text{ns}^{-1}$, $\alpha = 3$, $\gamma = 1\text{ns}^{-1}$, $\gamma_a = 0.1\text{ns}^{-1}$, $\gamma_s = 50\text{ns}^{-1}$, $\gamma_p = 10\text{ns}^{-1}$, $\beta_{sp} = 10^{-6}\text{ns}^{-1}$, $\tau = 7$ns, and $\tau_c = 4$ns. Time-step in the simulation was 2 ps.

Completely synchronized solutions of the rate equations (Eqs. (1)-(8)) exist only if the VCSELs are identical, and $f = \eta$ [38]. In this situation, the intensities of both of the LP modes of VCSELs are related by $I_{x,y}^s(t) = I_{x,y}^m(t+\tau-\tau_c)$, where $I_{x,y}^m = |E_{x,y}^m|^2$ and $I_{x,y}^s = |E_{x,y}^s|^2$. Here, $E_{x,y}^m$ and $E_{x,y}^s$ are optical fields of the VCSELs and related by $E_{x,y}^m(t-\tau_c)exp[-i(\omega\tau_c)] = E_{x,y}^s(t-\tau)exp[-i(\omega\tau)]$ for the perfect synchronization condition [39]. And if $\tau > \tau_c$ anticipation is possible. On the other hand, for $\eta > f$ injection-locking condition can be achieved between the VCSELs intensities and are related by $I_{x,y}^s(t) = I_{x,y}^m(t-\tau_c)$, where slave will lag master by τ_c time.

III. ANTICIPATION IN SYNCHRONIZATION AND CHARACTERIZATION

With the set of VCSEL parameters listed in Sec. II, and as a result of the external cavity optical feedback, ML exhibits chaos in its two linearly polarized modes (x and y). The chaotic output of ML is then injected into SL by polarization-preserved optical injection. For $\tau > \tau_c$ (i.e., $\tau = 7$ns and $\tau_c = 4$ns), $\eta = f$, $\Delta f = 0$, and other identical parameters of VCSELs, anticipatory synchronization obtained between ML and SL. We considered $\tau > \tau_c$ condition throughout this paper. The time traces of both x-LP and y-LP mode output intensity ($I_x^{m,s} = |E_x^{m,s}|^2$, $I_y^{m,s} = |E_y^{m,s}|^2$) of ML and SL are shown in Fig. 1. Keeping $\mu = 1.3$ and $\eta = f = 25\text{ns}^{-1}$, anticipated synchronization occurs between ML and SL in both x-LP mode intensity (Fig. 1(a1)) and y-LP mode intensity (Fig. 1(a2)). The anticipation nature can be clearly visualized by looking at the turn-on dynamics of master and slave lasers which are shown in Fig. 1(b1) (x-LP mode intensity) and Fig. 1(b2) (y-LP mode intensity). The parameters are maintained same as in Fig. 1(a1)-(a2). We can observe that, the VCSELs emit the first pulse nearly at the same time. The ML and SL pulses get influenced with steady state, by the optical feedback at the time after τ and by the injection at the time after τ_c, respectively. For the moderate injection rate, the SL will respond as similar to ML, but it will behave at the time τ_c whereas the ML will respond at the time τ [39]. From the Fig. 1(b1) (x-LP intensity) and Fig. 1(b2) (y-LP intensity), it is clearly evident that, soon after the initial pulse, the slave output started anticipating the master laser output. Additionally, the anticipation synchronization observed for higher bias current and larger injection/feedback rate. Maintaining $\mu = 1.7$ and $\eta = f = 37\text{ns}^{-1}$, Fig. 1(c1) and 1(c2) show the x-LP mode and y-LP mode output intensities, respectively. We can observe that at higher feedback rate and current, the output intensity fluctuations become larger in both LP mode components of the VCSELs.

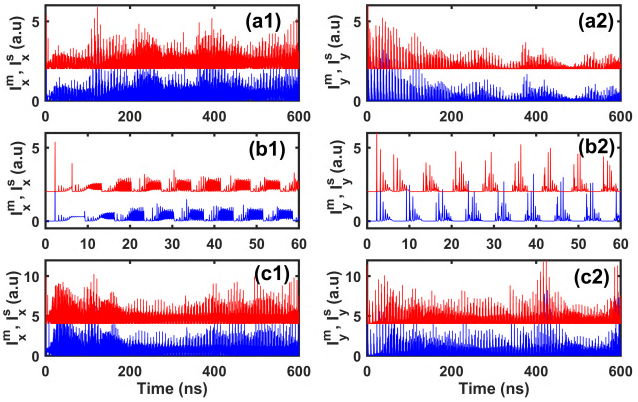

FIGURE 1. Time traces of ML (blue) and SL (red) for both x-LP and y-LP mode intensity for keeping $\tau = 7$ns and $\tau_c = 4$ns. SL intensity has been vertically shifted for the clarity. (a1) and (a2) correspond to x-LP and y-LP modes, respectively, for $\mu = 1.3$ and $\eta = f = 25\text{ns}^{-1}$. (b1) and (b2) Simultaneous turn-on dynamics of VCSELs of x-LP and y-LP modes, respectively. The VCSELs parameters are same as in Fig. 1(a1)-(a2). (c1) and (c2) correspond to x-LP and y-LP modes, respectively, for $\mu = 1.7$ and $\eta = f = 37\text{ns}^{-1}$.

The quality of synchronization and the lag time between VCSELs can be estimated by calculating cross-correlation (CC) function. The following cross-correlation coefficients C_x and C_y in terms of time-shift (Δt) are

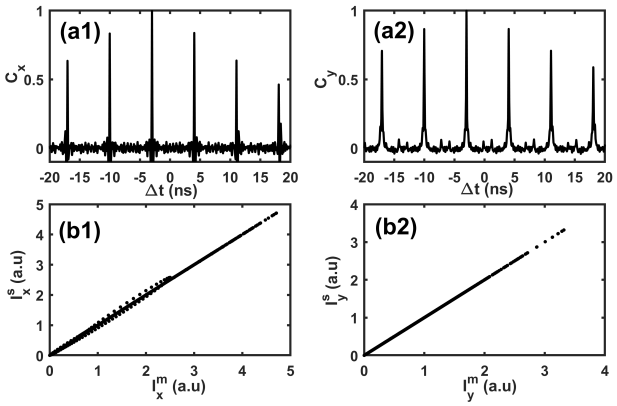

FIGURE 2. Cross correlation coefficients as a function of time shift and the synchronization plots between the respective LP mode component of ML and SL for keeping $\mu = 1.3$ and $\eta = f = 25\text{ns}^{-1}$. (a1) and (a2) CC coefficients of x-LP and y-LP mode outputs of VCSELs, respectively. (b1) and (b2) synchronization between ML and SL intensity for both LP modes.

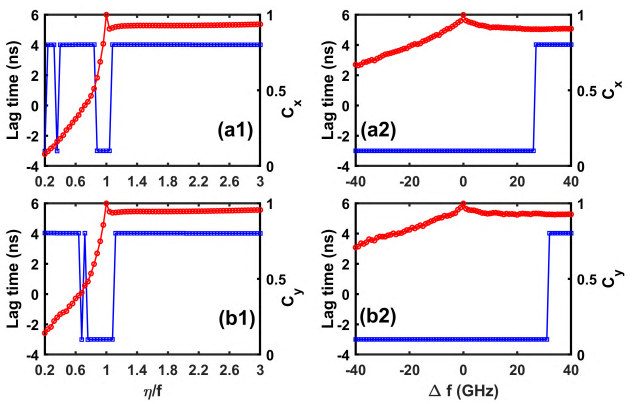

FIGURE 3. Evolution of correlation coefficients (red curves) and lag time (blue curves) as a function of injection rate η and frequency detuning Δf. (a1) and (a2) C_x and lag time between x-LP mode intensity as a function η and Δf, respectively. (b1) and (b2) C_y and lag time between y-LP mode intensity as a function η and Δf, respectively. For (a1) and (b1), Δf is 0. For (a2) and (b2), $\eta = f$ is 25ns^{-1}. Injection rate is scaled as η/f.

calculated by performing CC between the respective LP mode intensity outputs of ML and SL,

$$C_x(\Delta t) = \frac{\langle [I_x^m(t-\Delta t) - \langle I_x^m\rangle][I_x^s(t) - \langle I_x^s\rangle]\rangle}{\sqrt{\langle [I_x^m(t-\Delta t) - \langle I_x^m\rangle]^2\rangle \langle [I_x^s(t) - \langle I_x^s\rangle]^2\rangle}} \quad (9)$$

$$C_y(\Delta t) = \frac{\langle [I_y^m(t-\Delta t) - \langle I_y^m\rangle][I_y^s(t) - \langle I_y^s\rangle]\rangle}{\sqrt{\langle [I_y^m(t-\Delta t) - \langle I_y^m\rangle]^2\rangle \langle [I_y^s(t) - \langle I_y^s\rangle]^2\rangle}} \quad (10)$$

C_x and C_y correspond to the CC coefficients of x-LP mode and y-LP mode output intensities, respectively. The angle brackets denote time averaging, and $I_{x,y}^{m,s} = |E_{x,y}^{m,s}|^2$ is the intensity output of the laser. In CC analysis plot, the prominent peak value evaluates the synchronization quality, and location of the peak corresponds to the lag time between ML and SL intensity output. Ideally, C_x and C_y would be 1 for perfectly synchronized condition. Fig. 2 present the CC coefficient as a function of time shift and synchronization plots between ML and SL intensities of respective LP mode components for keeping $\mu = 1.3$, $\eta = f = 25\text{ns}^{-1}$, external-cavity feedback time $\tau = 7$ns, and coupling time $\tau_c = 4$ns. Figs. 2(a1) and 2(a2) show the CC function when there is an almost anticipated synchronization ($C_{x,y} > 0.997$) in both x-LP and y-LP mode components of VCSELs, respectively. The CC shows a maximum peak at the lag time -3ns. Since the lag time value is negative, the slave laser anticipates the chaotic dynamics of the master laser. The synchronization plot between x-LP mode component intensity of ML and SL is shown in Fig. 2(b1), and for the y-LP mode components is shown Fig. 2(b2). The synchronization plots have been plotted after considering the lag time between the ML and SL.

Next, we study the influences of injection rate and frequency detuning on the properties of synchronization in both x-LP and y-LP mode intensities of VCSELs. For our further discussions in this paper, we keep $\mu = 1.3$, $\tau = 7$ns, $\tau_c = 4$ns, and $f = 25\text{ns}^{-1}$. Fig. 3 displays the evolution of synchronization quality (red curves) and the lag time (blue curves) between the ML and SL intensities of both LP mode components. Figs. 3(a1) and 3(a2) correspond to the evolution of C_x and lag time between x-LP mode components of VCSELs intensities when we scan the injection rate η and frequency detuning Δf, respectively. Similarly, Figs. 3(b1) and 3(b2) represent the results for y-LP mode component of the VCSELs. Injection rate is scaled as η/f. From Figs. 3(a1) (for x-LP mode) and 3(b1) (for y-LP mode), when the injection rate η is less than the feedback rate f, we found very poor quality of synchronization between ML and SL for both of the LP mode components. The associated lag time fluctuates for lower injection rate due to the unstable coupling of SL with the ML. At $\eta = f$, perfect anticipatory synchronization occurs between ML and SL with a lag time -3ns, in both LP mode intensities. Anticipation regime prolonged for a small increase in η, i.e, up to $\eta/f = 1.1$ ($\eta/f = 1.28$) for x-LP(y-LP) mode intensities. As noticed in Fig. 1, the y-LP mode intensities fluctuations are less as compared with x-LP mode intensity fluctuations. Hence, as compared with x-LP mode, prefect synchronization between y-LP mode intensities has maintained up to slightly higher injection rates. And further increasing η, injection-locking synchronization regime arises between lasers, because at higher injection, the injected signal dominates the dynamics and has eventually suppressed all independent emission in the slave laser. Here SL output lags behind ML output by the time equal to coupling time τ_c which is 4ns.

Figs. 3(a2) (x-LP mode) and 3(b2) (y-LP mode), correspond to the influence of frequency detuning Δf on anticipation synchronization regime. As noticed that, anticipation synchronization is sensitive with the Δf variation. C_x and C_y are decreased and synchronization between ML and SL intensities for both LP modes ($C_{x,y}$) degrades drastically for a negative detuning Δf, whereas for positive detuning, although perfectly synchronized condition is lost, but maintains a good quality of synchronization between coupled VCSELs (Fig. 3(a2) and (b2)). In both x-LP and y-LP mode cases,

the perfect synchronization quality is lost between coupled VCSELs when $\Delta f > \pm 3$GHz. The synchronization switches from anticipation to injection-locking regime beyond $\Delta f > +25$GHz ($\Delta f > +30$GHz) in x-LP mode (y-LP mode). As discussed earlier in injection rate case, due to low intensity fluctuations in y-LP mode, perfect synchronization sustained in y-LP mode intensities for little higher positive detuning as compared with the x-LP mode intensities. The effect of detuning on the synchronization is presumably comparable to the previously discussed results of edge-emitting semiconductor lasers [35].

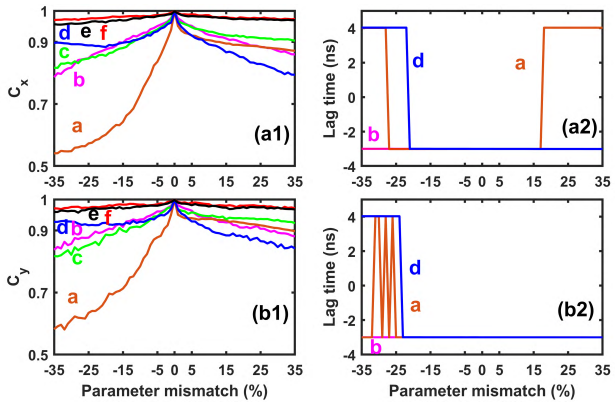

FIGURE 4. Evolution of correlation coefficient C_x (a1), C_y (b1), lag time between x-LP mode intensities of VCSELs (a2), and lag time between y-LP mode intensities of VCSELs (b2) against laser's intrinsic parameter mismatch in synchronization between ML and SL. Trace a: α, trace b: κ, trace c: γ_p, trace d: γ, trace e: γ_s, and trace f: γ_a correspond to the respective parameter mismatch.

In practice, it is quite impossible to obtain the precisely same parameters of two lasers. The parameter mismatches will have an influence in the chaos synchronization [34]. We discuss the effect of internal parameter mismatches between ML and SL on the anticipated chaos synchronization in both LP mode intensities in order to estimate the robustness of chaos synchronization. We keep $\eta = f = 25\text{ns}^{-1}$, $\Delta f = 0$, $\tau = 7$ns and $\tau_c = 4$ns. The relative parameter mismatch can be defined as follows, $\Delta p = (p_s - p_m)/p_m$ where p represent the internal parameters such as, κ, α, γ_a, γ_p, γ_s and γ. From CC analysis between ML and SL, the quality of synchronization (C_x and C_y) characterized for both x-LP and y-LP mode intensities. The variations of correlation coefficient value of x-LP mode intensities C_x and the corresponding lag time are shown in Fig. 4(a1) and 4(a2), respectively, against the mismatched parameters. Similarly, the effect of parameter mismatch on the synchronization of y-LP mode intensity (C_y) and between coupled VCSELs is shown in Fig. 4(b1) and the corresponding lag time is presented in Fig. 4(b2). We observed from the Fig. 4(a1) and (b1) that, the impact of cavity dichroism γ_a (trace f) and spin-flip relaxation rate γ_s (trace e), are fairly limited, C_x and C_y show a moderate variation and anticipatory synchronization is preserved for both parameters mismatch $\Delta\gamma_s$ and $\Delta\gamma_a$ variations. For these parameters, the synchronization is robust even after $\pm 20\%$ mismatch. Whereas other parameters such as the carrier decay rate γ (trace d), birefringence γ_p (trace c), photon decay rate κ (trace b), and linewidth enhancement factor α (trace a) appear to be the critical parameters. For these parameters, there is a degradation of the perfect synchronization quality in both LP mode cases (C_x and C_y) as the parameter mismatch increases (see Fig. 4(a1) and (b1)).

We noticed asymmetries in synchronization quality between negative and positive mismatch for parameters such as γ (trace d), γ_p (trace c), α (trace a). It is found that, α will be easily lost the perfect synchronization quality for a negative mismatch. In x-LP mode component, for $\Delta\alpha > +18\%$ and $\Delta\alpha > -23\%$, the anticipation synchronization switches to injection-locking regime with lag time equal to 4ns, which is τ_c (trace a in Fig. 4(a2)). In the case of y-LP mode, above -25% of $\Delta\alpha$ the regime jumps between anticipation and injection-locking synchronization (Fig. 4(b2)). However it is noted in both LP mode cases that the quality of synchronization is poor for negative mismatch of α parameter. In Fig. 4(a1) and (b1), $C_{x,y}$ show degradation for a positive parameter mismatch of γ (trace d). Also, in both LP modes synchronization switches to injection-locking regime from anticipation for negative mismatched parameter beyond -23% (Figs. 4(a2) and 4(b2)). In the γ_p (trace c) parameter, negative mismatch affects the anticipated synchronization quality in both LP modes. As seen in the Figs. 4(a1) and 4(b1) that the $C_{x,y}$ value reduced with a same manner against increasing positive and negative mismatch of the parameter κ (trace b). Similar to the κ parameter mismatch effect on lag time (trace b in Figs. 4(a2) and 4(b2)), the lag time maintained at -3ns for γ_p, γ_s, and γ_a parameter mismatches. From these results we understand that, mismatches between the ML and SL parameters would also lead a synchronization regimes switching from anticipation to injection-locking synchronization. However, the quality of chaos synchronization will degrade above $\pm 20\%$ mismatches in critical parameters such as α, κ, γ_p, and γ.

IV. MAPPING OF CORRELATION COEFFICIENT AND LAG TIME IN INJECTION RATE AND PARAMETER MISMATCH SPACE

In the preceding section, we detailed the influences of injection parameters (η and Δf) on the nature anticipation synchronization in coupled VCSELs. We also discussed the effect of intrinsic parameter mismatches on synchronization regimes and quality. We observed switching of synchronization regime from anticipation to injection-locking against mismatch variation of certain intrinsic parameters.

In this section, we analyze the anticipation synchronization properties and switching of synchronization regime on the injection rate η and parameter mismatch Δp plane, for both x-LP and y-LP mode intensities of VCSELs. We addressed this analysis in order to identify the switching of anticipation to injection-locking regimes and the evolution of synchronization quality in $[\eta/f, \Delta p]$ plane.

We keep $\mu = 1.3$, $f = 25\text{ns}^{-1}$, $\Delta f = 0$, $\tau = 7$ns, and $\tau_c = 4$ns for our discussion. Fig. 5 shows the

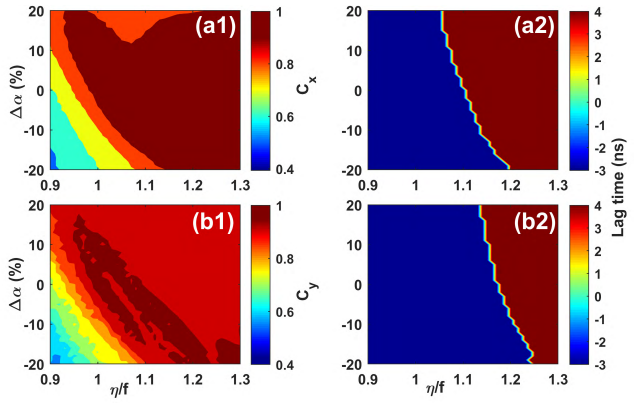

FIGURE 5. Mapping of maximal correlation coefficients (C_x and C_y) and the associated lag time between ML and SL intensities in the plane of injection rate η/f and α parameter mismatch. (a1)-(a2) C_x and lag time between x-LP mode intensities of ML and SL. (b1)-(b2) C_y and lag time between y-LP mode intensities of ML and SL.

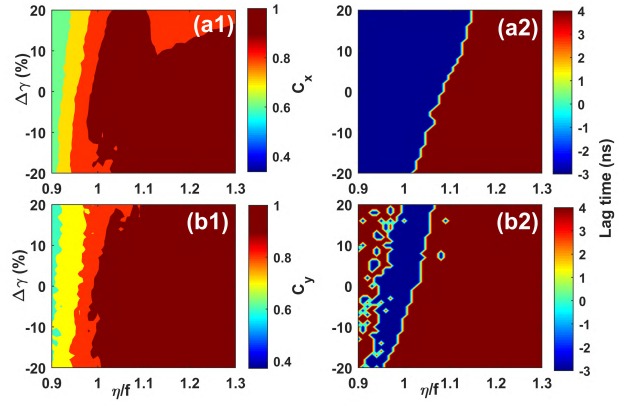

FIGURE 6. Mapping of C_x, C_y, and the associated lag time between ML and SL intensities in the plane of η/f and γ parameter mismatch. (a1)-(a2) C_x and lag time between x-LP mode intensities of ML and SL. (b1)-(b2) C_y and lag time between y-LP mode intensities of ML and SL.

maximum cross correlation coefficients map and the associated lag time in the $[\eta/f, \Delta\alpha]$ plane. Fig. 5(a1) correspond to C_x evolution (x-LP mode) and the associated lag time is shown in Fig. 5(a2). Evolution of C_y (for y-LP mode) and corresponding lag time are shown in Figs. 5(b1) and 5(b2), respectively. The dark red boundaries in Figs. 5(a1) and 5(b1) indicate a good synchronization quality ($C_{x,y} > 0.9$) has been observed between ML and SL intensities for an adequately large injection rates. In both LP modes (Fig. 5(b1) and 5(b2)), anticipation maintained at the higher value boundaries of η/f and larger negative mismatch of α parameter. When $\Delta\alpha$ is positive, synchronization switches to injection-locking regime for $\eta/f > 1.15$. In this case the nature of synchronization quality and regime changeover are occurred nearly at the same $[\eta/f, \Delta\alpha]$ boundaries for both LP mode components.

Mapping of $C_{x,y}$ and the associated lag time between ML and SL's LP mode intensities for $[\eta/f, \Delta\gamma]$ plane are shown in Fig. 6. As noticed from the Figs. 6(a1) and 5(b1) that there is a wide span of quality of synchronization boundaries for both x-LP and y-LP modes. However, the anticipation synchronization regime is limited for the both LP mode cases (Figs. 6(a2) and 5(b2)). In x-LP mode case, injection-locking

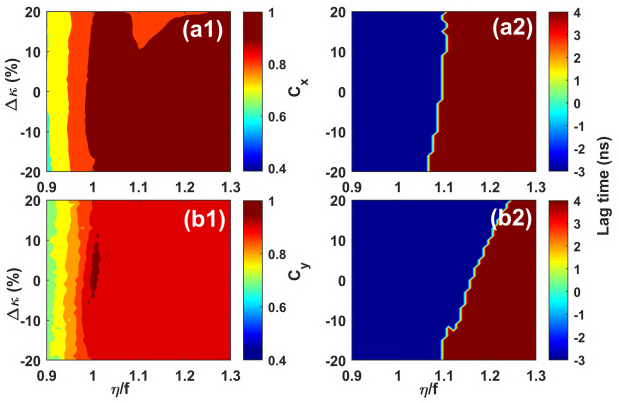

FIGURE 7. Mapping of C_x, C_y, and the associated lag time between ML and SL intensities in the plane of η/f and κ parameter mismatch. (a1)-(a2) C_x and lag time between x-LP mode intensities of ML and SL. (b1)-(b2) C_y and lag time between y-LP mode intensities of ML and SL.

regime with lag time 4ns arises for above $\eta/f > 1.05$ with higher negative mismatch of γ parameter boundaries and is shown in Fig. 6(a2). Additionally, for a positive mismatch of γ, although synchronization quality is not perfect, anticipation with lag time -3ns preserved up to the η/f value abound 1.15. Whereas in the y-LP mode case, anticipation retains within a limited area of $[\eta/f, \Delta\gamma]$ plane and is indicated as blue region in Fig. 6(b2).

Fig. 7 shows the analysis of maximum correlation coefficients and associated lag time evolution, in the synchronization between ML and SL intensities for both x-LP and y-LP mode components, in the $[\eta/f, \Delta\kappa]$ plane. In x-LP mode synchronization between ML and SL, C_x covers broad region in $[\eta, \Delta\kappa]$ space of larger value of η and parameter mismatch of κ within $\pm 20\%$ and is shown in Fig. 7(a1). In this x-LP mode case the synchronization regime switches to injection-locking from anticipation for $\eta/f > 1.12$ which is shown in Fig. 7(a2). In the case of y-LP mode synchronization, the synchronization quality C_y bound within a small region (Fig. 7(b1)) resembles that increasing η and $\Delta\kappa$ would decrease the quality. The red region in the Fig. 7(b1) shows that $C_y > 0.8$ but less than 0.9. Fig. 7(b2) shows that for a positive mismatch of κ parameter, injection-locked type synchronization arises only after $\eta/f > 1.25$ condition, but in the negative mismatch its arises after $\eta/f > 1.09$.

The dependency of synchronization quality $C_{x,y}$ and corresponding lag time between ML and SL intensities in the $[\eta/f, \Delta\gamma_p]$ plane, for both x-LP and y-LP mode cases are shown in Fig. 8. It is evident from the Figs. 8(a1) and 8(b1) that, beyond $\eta/f > 1$ the synchronization quality of x-LP (C_x) and y-LP (C_y) modes found better and mismatch in the parameter γ_p is less significant in affecting the C_x and C_y value. Moreover, an increase of η affects the anticipated synchronization and switches to injection-locking regime with lag time 4ns over $\eta/f > 1.1$ ($\eta/f > 1.06$) value for the x-LP (y-LP) mode intensity of synchronization between ML and SL (see Figs. 8(a2) and 8(b2)).

Evolution of $C_{x,y}$ and the respective lag time in $[\eta/f, \Delta\gamma_s]$ plane are shown in Fig. 9 for both LP modes of

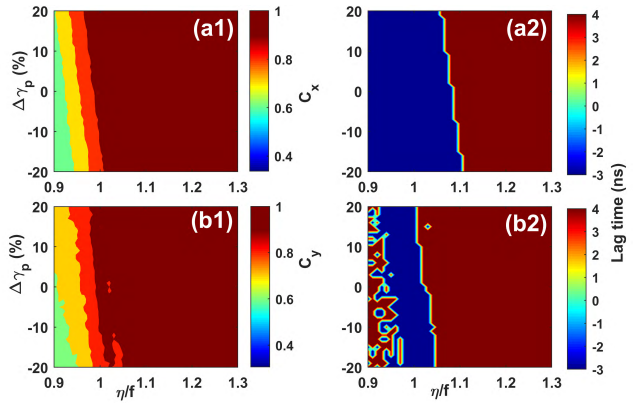

FIGURE 8. Mapping of C_x, C_y, and the associated lag time between ML and SL intensities in the plane of η/f and γ_p parameter mismatch. (a1)-(a2) C_x and lag time between x-LP mode intensities of ML and SL. (b1)-(b2) C_y and lag time between y-LP mode intensities of ML and SL.

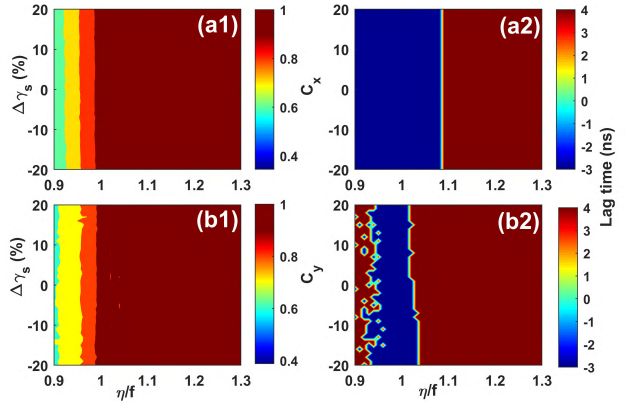

FIGURE 9. Mapping of C_x, C_y, and the associated lag time between ML and SL intensities in the plane of η/f and γ_s parameter mismatch. (a1)-(a2) C_x and lag time between x-LP mode intensities of ML and SL. (b1)-(b2) C_y and lag time between y-LP mode intensities of ML and SL.

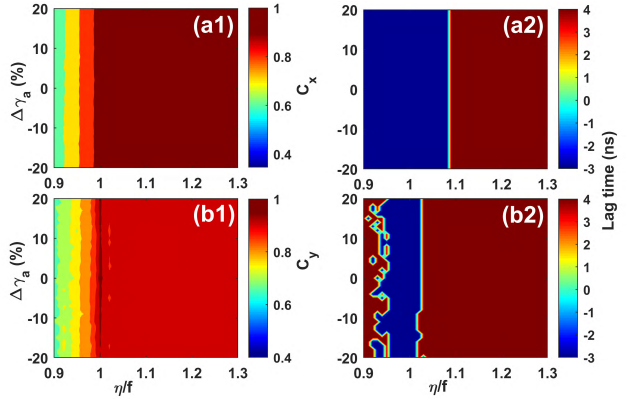

FIGURE 10. Mapping of C_x, C_y, and the associated lag time between ML and SL intensities in the plane of η/f and γ_a parameter mismatch. (a1)-(a2) C_x and lag time between x-LP mode intensities of ML and SL. (b1)-(b2) C_y and lag time between y-LP mode intensities of ML and SL.

coupled VCSELs. The mapping of $C_{x,y}$ and associated lag time in $[\eta/f,\ \Delta\gamma_a]$ plane are shown in Fig. 10. As we have already observed from the response of $C_{x,y}$ over parameter mismatch that, mismatches in γ_s (trace e) and γ_a (trace f) parameters found to influence less in the synchronization quality $C_{x,y}$ (Figs. 4(a1) and 4(b1)). Hence, while varying the mismatch same trend of $C_{x,y}$ has been found to occur in Fig. 9 and Fig. 10 for γ_s and γ_a parameters, respectively. Besides, synchronization switches from anticipation to injection-locking regime over η. It is found Fig. 9(b1) and 10(b1) that for x-LP mode case synchronization regime switch occur after $\eta/f > 1.09$ for both parameters γ_s and γ_a, respectively. In the case of y-LP mode, regime switches after $\eta/f > 1.01$ for γ_s and γ_a parameters which are shown in Fig. 9(b2) and 10(b2), respectively. The correlation coefficient $C_{x,y}$ values from 0.4 to 0.75 correspond to the color variations from blue to yellow in all mapping figures.

The mapping of synchronization quality $C_{x,y}$ and examining synchronization regimes in the plane of injection rate η and laser's internal parameters mismatch Δp ($[\eta/f\ \ \Delta p]$ plane) reveal the following observations. For parameters such as α, γ, and κ, even for higher values of η, perfectly anticipation synchronization preserved between ML and SL in both LP modes (x-LP and y-LP) or any one of the modes. It is essentially due to the mismatched parameters effect. Irrespective of the synchronization switching from anticipation to injection-locking regime, in $[\eta/f,\ \Delta p]$ plane, a good quality of synchronization boundaries occurred for the higher injection rates. This analysis suggests that perfect synchronization is possible in experiments even if the unavoidable parameter mismatch exist in certain parameters such as α, γ, κ and γ_p.

V. CONCLUSIONS

To conclude, we have numerically studied the anticipated chaos synchronization in the two uni-directionally coupled VCSELs by considering the configurations of a master laser with the isotropic optical feedback and polarization-preserved optical injection to slave laser. By the cross-correlation analysis between master and slave laser intensities, a synchronization quality and lag time between lasers are calculated. Our results show that, a regime of anticipatory synchronization obtained in which slave dynamics anticipates master by the $\tau - \tau_c$ when $\tau > \tau_c$ and $\eta = f$. The anticipation is robust but not perfectly synchronized to a small variation of injection rates, frequency detunings and parameter mismatches. Also the results show a regime of injection-locking synchronization between master and slave lasers, in which slave lags behind master with τ_c time for higher injection rates and in a certain parameter mismatch. The mapping results of synchronization quality and associated lag time in $[\eta/f,\ \Delta p]$ plane suggest that, for parameters such as α, γ, and κ, even for higher values of η, perfectly anticipation synchronization arises between master and slave in both linearly polarized or in any one of the modes which is due to the mismatch effect. In $[\eta/f,\ \Delta p]$ plane, a good quality of synchronization boundaries occurred for the higher injection rates irrespective of synchronization regime change.

REFERENCES

[1] R. Michalzik, *VCSELs: Fundamentals, Technology and Applications of Vertical-Cavity Surface-Emitting Lasers*. Berlin, Germany: Springer-Verlag, 2013.

[2] M. S. Miguel, Q. Feng, and J. V. Moloney, "Light-polarization dynamics in surface-emitting semiconductor lasers," *Phys. Rev. A, Gen. Phys.*, vol. 52, no. 2, pp. 1728–1739, Aug. 1995.

[3] J. Martin-Regalado, M. S. Miguel, N. B. Abraham, and F. Prati, "Polarization switching in quantum-well vertical-cavity surface-emitting lasers," *Opt. Lett.*, vol. 21, no. 5, pp. 351–353, Mar. 1996.

[4] K. Panajotov, B. Ryvkin, J. Danckaert, M. Peeters, H. Thienpont, and I. Veretennicoff, "Polarization switching in VCSEL's due to thermal lensing," *IEEE Photon. Technol. Lett.*, vol. 10, no. 1, pp. 6–8, Jan. 1998.

[5] C. Masoller and N. B. Abraham, "Low-frequency fluctuations in vertical-cavity surface-emitting semiconductor lasers with optical feedback," *Phys. Rev. A, Gen. Phys.*, vol. 59, pp. 3021–3031, Apr. 1999.

[6] K. D. Choquette, D. A. Richie, and R. E. Leibenguth, "Temperature dependence of gain-guided vertical-cavity surface emitting laser polarization," *Appl. Phys. Lett.*, vol. 64, no. 16, pp. 2062–2064, 1994.

[7] J. Martin-Regalado, F. Prati, M. S. Miguel, and N. B. Abraham, "Polarization properties of vertical-cavity surface-emitting lasers," *IEEE J. Quantum Electron.*, vol. 33, no. 5, pp. 765–783, May 1997.

[8] B. Ryvkin *et al.*, "Effect of photon-energy-dependent loss and gain mechanisms on polarization switching in vertical-cavity surface-emitting lasers," *J. Opt. Soc. Amer. B, Opt. Phys.*, vol. 16, no. 11, pp. 2106–2113, Nov. 1999.

[9] C. Masoller and N. B. Abraham, "Polarization dynamics in vertical-cavity surface-emitting lasers with optical feedback through a quarter-wave plate," *Appl. Phys. Lett.*, vol. 74, no. 8, pp. 1078–1080, Feb. 1999.

[10] B. Nagler *et al.*, "Polarization-mode hopping in single-mode vertical-cavity surface-emitting lasers: Theory and experiment," *Phys. Rev. A, Gen. Phys.*, vol. 68, pp. 013813-1–013813-8, Jul. 2003.

[11] N. C. Gerhardt and M. R. Hofmann, "Spin-controlled vertical-cavity surface-emitting lasers," *Adv. Opt. Technol.*, vol. 2012, pp. 268949-1–268949-15, Dec. 2011.

[12] A. Valle, L. Pesquera, and K. A. Shore, "Polarization selection and sensitivity of external cavity vertical-cavity surface-emitting laser diodes," *IEEE Photon. Technol. Lett.*, vol. 10, no. 5, pp. 639–641, May 1998.

[13] A. Tabaka *et al.*, "Dynamics of vertical-cavity surface-emitting lasers in the short external cavity regime: Pulse packages and polarization mode competition," *Phys. Rev. A, Gen. Phys.*, vol. 73, pp. 013810-1–013810-14, Jan. 2006.

[14] Z. G. Pan, S. Jiang, and M. Dagenais, "Optical injection induced polarization bistability in vertical-cavity surface-emitting lasers," *Appl. Phys. Lett.*, vol. 63, no. 22, pp. 2999–3001, Nov. 1993.

[15] M. Sciamanna and K. Panajotov, "Route to polarization switching induced by optical injection in vertical-cavity surface-emitting lasers," *Phys. Rev. A, Gen. Phys.*, vol. 73, pp. 023811-1–023811-17, Feb. 2006.

[16] A. Valle, L. Pesquera, S. I. Turovets, and J. M. Lopez, "Nonlinear dynamics of current-modulated vertical-cavity surface-emitting lasers," *Opt. Commun.*, vol. 208, pp. 173–182, Jul. 2002.

[17] M. Sciamanna, A. Valle, P. Megret, M. Blondel, and K. Panajotov, "Nonlinear polarization dynamics in directly modulated vertical-cavity surface-emitting lasers," *Phys. Rev. E, Stat. Phys. Plasmas Fluids Relat. Interdiscip. Top.*, vol. 68, pp. 016207-1–016207-4, Jul. 2003.

[18] M. W. Lee, Y. Hong, and K. A. Shore, "Experimental demonstration of VCSEL-based chaotic optical communications," *IEEE Photon. Technol. Lett.*, vol. 16, no. 10, pp. 2392–2394, Oct. 2004.

[19] M. Sciamanna and K. A. Shore, "Physics and applications of laser diode chaos," *Nature Photon.*, vol. 9, pp. 151–162, Feb. 2015.

[20] N. Jiang, C. Xue, D. Liu, Y. Lv, and K. Qiu, "Secure key distribution based on chaos synchronization of VCSELs subject to symmetric random-polarization optical injection," *Opt. Lett.*, vol. 42, pp. 1055–1058, Mar. 2011.

[21] J. Ke, L. Yi, G. Q. Xia, and W. Hu, "Chaotic optical communications over 100-km fiber transmission at 30-Gb/s bit rate," *Opt. Lett.*, vol. 43, pp. 1323–1326, Mar. 2018.

[22] A. Argyris *et al.*, "Chaos-based communications at high bit rates using commercial fibre-optic links," *Nature*, vol. 438, pp. 343–346, Nov. 2005.

[23] Y. Hong, M. W. Lee, and K. A. Shore, "Optimised message extraction in laser diode based optical chaos communications," *IEEE J. Quantum Electron.*, vol. 46, no. 2, pp. 253–257, Feb. 2010.

[24] V. Annovazzi-Lodi, G. Aromataris, M. Benedetti, and S. Merlo, "Private message transmission by common driving of two chaotic lasers," *IEEE J. Quantum Electron.*, vol. 46, no. 2, pp. 258–264, Feb. 2010.

[25] L. M. Pecora and T. L. Carroll, "Synchronization in chaotic systems," *Phys. Rev. Lett.*, vol. 64, no. 8, pp. 821–824, Feb. 1990.

[26] T. Sugawara, M. Tachikawa, T. Tsukamoto, and T. Shimizu, "Observation of synchronization in laser chaos," *Phys. Rev. Lett.*, vol. 72, pp. 3502–3505, May 1994.

[27] R. Roy and K. S. Thornburg, Jr., "Experimental synchronization of chaotic lasers," *Phys. Rev. Lett.*, vol. 72, pp. 2009–2012, Mar. 1994.

[28] G. D. VanWiggeren and R. Roy, "Communication with chaotic lasers," *Science*, vol. 279, pp. 1198–1200, Feb. 1998.

[29] D. Y. Tang, R. Dykstra, M. W. Hamilton, and N. R. Heckenberg, "Observation of generalized synchronization of chaos in a driven chaotic system," *Phys. Rev. E, Stat. Phys. Plasmas Fluids Relat. Interdiscip. Top.*, vol. 57, pp. 5247–5251, May 1998.

[30] A. Uchida, M. Shinozuka, T. Ogawa, and F. Kannari, "Experiments on chaos synchronization in two separate microchip lasers," *Opt. Lett.*, vol. 24, pp. 890–892, Jul. 1999.

[31] S. Sivaprakasam and K. A. Shore, "Demonstration of optical synchronization of chaotic external-cavity laser diodes," *Opt. Lett.*, vol. 24, pp. 466–468, Apr. 1999.

[32] Y. Hong, M. W. Lee, P. S. Spencer, and K. A. Shore, "Synchronization of chaos in unidirectionally coupled vertical-cavity surface-emitting semiconductor lasers," *Opt. Lett.*, vol. 29, pp. 1215–1217, Jun. 2004.

[33] N. Fujiwara, Y. Takiguchi, and J. Ohtsubo, "Observation of the synchronization of chaos in mutually injected vertical-cavity surface-emitting semiconductor lasers," *Opt. Lett.*, vol. 28, pp. 1677–1679, Sep. 2003.

[34] H. F. Chen and J. M. Liu, "Open-loop chaotic synchronization of injection-locked semiconductor lasers with gigahertz range modulation," *IEEE J. Quantum Electron.*, vol. 36, no. 1, pp. 27–34, Jan. 2000.

[35] A. Locquet, C. Masoller, and C. R. Mirasso, "Synchronization regimes of optical-feedback-induced chaos in unidirectionally coupled semiconductor lasers," *Phys. Rev. E, Stat. Phys. Plasmas Fluids Relat. Interdiscip. Top.*, vol. 65, pp. 056205-1–056205-12, Apr. 2002.

[36] J. Ohtsubo, "Chaos synchronization and chaotic signal masking in semiconductor lasers with optical feedback," *IEEE J. Quantum Electron.*, vol. 38, no. 9, pp. 1141–1154, Sep. 2002.

[37] H. U. Voss, "Anticipating chaotic synchronization," *Phys. Rev. E, Stat. Phys. Plasmas Fluids Relat. Interdiscip. Top.*, vol. 61, pp. 5115–5119, May 2000.

[38] V. Ahlers, U. Parlitz, and W. Lauterborn, "Hyperchaotic dynamics and synchronization of external-cavity semiconductor lasers," *Phys. Rev. E, Stat. Phys. Plasmas Fluids Relat. Interdiscip. Top.*, vol. 58, pp. 7208–7213, Dec. 1998.

[39] C. Masoller, "Anticipation in the synchronization of chaotic semiconductor lasers with optical feedback," *Phys. Rev. Lett.*, vol. 86, pp. 2782–2785, Mar. 2001.

[40] S. Sivaprakasam, E. M. Shahverdiev, P. S. Spencer, and K. A. Shore, "Experimental demonstration of anticipating synchronization in chaotic semiconductor lasers with optical feedback," *Phys. Rev. Lett.*, vol. 87, pp. 154101-1–154101-3, Sep. 2001.

[41] Y. Liu, Y. Takiguchi, P. Davis, and S. Saito, "Experimental observation of complete chaos synchronization in semiconductor lasers," *Appl. Phys. Lett.*, vol. 80, pp. 4306–4308, Apr. 2002.

[42] P. S. Spencer, C. R. Mirasso, P. Colet, and K. A. Shore, "Modeling of optical synchronization of chaotic external-cavity VCSELs," *IEEE J. Quantum Electron.*, vol. 34, no. 9, pp. 1673–1679, Sep. 1998.

[43] M. S. Torre, C. Masoller, and K. A. Shore, "Synchronization of unidirectionally coupled multi-transverse-mode vertical-cavity surface-emitting lasers," *J. Opt. Soc. Amer. B, Opt. Phys.*, vol. 21, pp. 1772–1780, Oct. 2004.

[44] I. Gatare, M. Sciamanna, A. Locquet, and K. Panajotov, "Influence of polarization mode competition on the synchronization of two unidirectionally coupled vertical-cavity surface-emitting lasers," *Opt. Lett.*, vol. 32, pp. 1629–1631, Jun. 2007.

[45] M. Sciamanna, I. Gatare, A. Locquet, and K. Panajotov, "Polarization synchronization in unidirectionally coupled vertical-cavity surface-emitting lasers with orthogonal optical injection," *Phys. Rev. E, Stat. Phys. Plasmas Fluids Relat. Interdiscip. Top.*, vol. 75, pp. 056213-1–056213-10, May 2007.

[46] Y. Hong, M. W. Lee, J. Paul, P. S. Spencer, and K. A. Shore, "Enhanced chaos synchronization in unidirectionally coupled vertical-cavity surface-emitting semiconductor lasers with polarization-preserved injection," *Opt. Lett.*, vol. 33, pp. 587–589, Mar. 2008.

[47] S. Xiang *et al.*, "Impact of unpredictability on chaos synchronization of vertical-cavity surface-emitting lasers with variable-polarization optical feedback," *Opt. Lett.*, vol. 36, pp. 3497–3499, Sep. 2011.

[48] D.-Z. Zhong, G.-Q. Xia, Z.-M. Wu, and X.-H. Jia, "Complete chaotic synchronization characteristics of the linear-polarization mode of vertical-cavity surface-emitting semiconductor lasers with isotropic optical feedback," *Opt. Commun.*, vol. 281, pp. 1698–1709, Mar. 2008.
[49] A. Quirce, A. Valle, H. Thienpont, and K. Panajotov, "Chaos synchronization in mutually coupled 1550-nm vertical-cavity surface-emitting lasers with parallel polarizations and long delay time," *J. Opt. Soc. Amer. B, Opt. Phys.*, vol. 33, pp. 90–98, Jan. 2016.
[50] A. Scire, J. Mulet, C. R. Mirasso, J. Danckaert, and M. S. Miguel, "Polarization message encoding through vectorial chaos synchronization in vertical-cavity surface-emitting lasers," *Phys. Rev. Lett.*, vol. 90, pp. 113901-1–113901-4, Mar. 2003.
[51] N. Jiang, W. Pan, B. Luo, W. Zhang, and D. Zheng, "Stable anticipation synchronization in mutually coupled vertical-cavity surface-emitting lasers system," *Chin. Opt. Lett.*, vol. 6, pp. 517–519, Jul. 2008.
[52] M. Ozaki *et al.*, "Leader-laggard relationship of chaos synchronization in mutually coupled vertical-cavity surface-emitting lasers with time delay," *Phys. Rev. E, Stat. Phys. Plasmas Fluids Relat. Interdiscip. Top.*, vol. 79, pp. 026210-1–026210-7, Feb. 2009.

ELUMALAI JAYAPRASATH was born in Kanchipuram, Tamilnadu, India, in 1988. He received the B.Sc. degree from the Loyola College, Chennai, India, in 2008, and the M.Sc. and Ph.D. degrees from Pondicherry University, Pondicherry, India, in 2010 and 2016, respectively, all in physics. His thesis work was on the propagation delay and synchronization of chaotic semiconductor lasers.

He is currently a Post-Doctoral Researcher with the School of Physics, Southwest University, Chongqing, China. His current research lies in the chaos synchronization of semiconductor lasers and its utilization for secure optical communications.

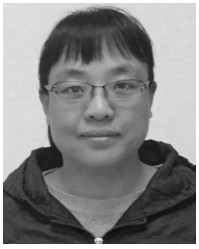

YU-SHUANG HOU was born in Tangshan, Hebei, China, in 1979. She received the M.Sc. degree in applied mathematics from Inner Mongolia University, Hohhot, China, in 2006. She is currently pursuing the Ph.D. degree in optics with Southwest University. Her current research mainly focuses on the photonic reservoir computing and its application.

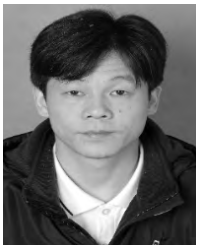

ZHENG-MAO WU was born in Wuyuan, Jiangxi, China, in 1970. He received the B.Sc., M.Sc. and Ph.D. degrees in optics from Sichuan University, Chengdu, Sichuan, China, in 1992, 1995, and 2003, respectively.

He is currently a Full Professor with the School of Physics, Southwest University, Chongqing, China. He has authored or co-authored over 100 publications. His current research interests include nonlinear dynamics of semiconductor lasers and their applications, chaotic semiconductor lasers and their applications.

GUANG-QIONG XIA was born in Fushun, Sichuan, China, in 1970. She received the B.Sc., M.Sc., and Ph.D. degrees in optics from Sichuan University, Chengdu, Sichuan, China, in 1992, 1995, and 2002, respectively.

She is currently a Full Professor with the School of Physics, Southwest University, Chongqing, China. She has authored or co-authored over 140 publications including about 100 journal papers. Her current research interests include nonlinear dynamics of semiconductor lasers, synchronization and control of chaotic semiconductor lasers, chaos secure communication based on semiconductor lasers, and microwave photonics.